Bistriazole-*p*-benzoquinone and its alkali salts: electrochemical behaviour in aqueous alkaline solutions†

H. Bunzen, * A. Lamp, M. Grzywa, C. Barkschat and D. Volkmer

Quinones are well known as redox-active compounds. In this work bistriazole-*p*-benzoquinone was prepared and its electrochemical behaviour in aqueous alkaline solutions was studied by cyclic voltammetry. Two successive one-electron reduction steps were observed – the first step was reversible and the second quasireversible. Based on the nature of the alkali cation, the potential of the cathodic peak minimum and the anodic peak maximum was shifted towards positive direction as follows $Li^+ > Na^+ > K^+$. In order to know more about the chemical structure of the alkali salts, the lithium, sodium and potassium salts of bistriazole-*p*-benzoquinone were crystallized and their structure could be revealed by single crystal X-ray analysis. Additionally, the thermal stability of the compounds was investigated by thermogravimetric analysis and variable temperature X-ray powder diffraction analysis.

Introduction

1,2,3-Triazoles and benzotriazoles are important types of heterocyclic compounds. They find numerous applications in industry and play a very important role in medicine and drug discovery.[1] Beyond this, these compounds are intensively studied due to their theoretical interest and synthetic usefulness.[2] They are stable to reduction and oxidation as well as to hydrolysis in acidic and basic conditions, which indicates their high aromatic stabilization. They have a high dipole moment (about 5D) and are able to participate actively in hydrogen bond formation as well as in dipole–dipole and π stacking interactions.[1c,3] In this work, the 1,2,3-triazole moiety was combined with a benzoquinone unit.

Quinones are one of the most important and well-studied examples of organic redox-active compounds.[4] They are well-represented in biological electron transport processes[5] and found a number of applications as dyes, and as oxidizing and reducing agents in chemical synthesis.[6] In addition, a number of quinones have also been found to have medicinal properties, including antibiotic and antitumor activity.[7] From a fundamental standpoint, quinones have played an important role in developing our current understanding of organic redox chemistry. The quinones (Q) undergo in organic aprotic media two successive one-electron reduction steps: $Q \rightarrow Q^{\bullet -} \rightarrow Q^{2-}$. This process can be observed by cyclic voltammetry where two reduction and two corresponding oxidation peaks are generated.[4] The first step is reversible and the second quasireversible. In a contrast to organic aprotic solvents, in aqueous solutions quinones undergo fast two-electron reduction with or without proton transfer depending on the pH value.[8] While there have been hundreds of electrochemical studies of quinones in aqueous solutions over the past 100+ years, almost all of these have been done in pH buffered solutions. Only several investigations have been done in unbuffered aqueous solution.[9]

Reversible quinone/hydroquinone couples have been reported as efficient energy harvesting and storage materials.[10] For instance, recently a metal-free flow battery based on the redox chemistry of 9,10-anthraquinone-2,7-disulphonic acid (AQDS) was introduced.[11] In another work, redox properties of hydroxy-substituted 9,10-antraquinones in a 1 M aqueous KOH solution were investigated and the use of the materials in alkaline flow batteries was demonstrated.[12] It was shown that the hydroxyl functional groups, when deprotonated, provided greater solubility and electron donation capability, which resulted in an increase in the open-circuit voltage. Herein we report on structurally similar bistriazole-*p*-benzoquinone. Triazoles have been previously used by our group to construct various coordination framework architectures.[13] They are strong N-donor ligands that can compete with abundant O-donor ligands such as the ubiquitous water molecule, if

Chair of Solid State and Materials Chemistry, Institute of Physics, University of Augsburg, Universitätsstraße 1, D-86159 Augsburg, Germany. E-mail: hana.bunzen@physik.uni-augsburg.de

† Electronic supplementary information (ESI) available: TGA, IR, NMR, VT-XRPD, solubility of H_2-btbq, cyclic voltammetry measurements at different scan rates, and X-ray single crystal analysis. CCDC 1561795–1561797. For ESI and crystallographic data in CIF or other electronic format see DOI: 10.1039/c7dt02803b

combined with late transition metal ions in particular. Moreover, bistriazolate ligands often coordinate in a multidentate fashion (μ_4- or μ_6-bridging mode) and, therefore seem to be appropriate anchor group for introducing redox-active moieties into coordination polymers. Since both, quinones as well as triazoles, are electron-poor organic units, an electrochemical study on the properties of fused systems containing both groups seems mandatory, which is one of the incentives for the studies presented here.

Results and discussion

Ligand synthesis

A preparation of bistriazole-*p*-benzoquinone (H_2-btbq, Scheme 1) starting from tetraamino-*p*-benzoquinone (**2**) was recently reported.[14] Herein we report on an alternative synthesis route which was adapted from the ref. 15 and optimized. As a starting material, it uses benzobistriazole (**1**) which was recently utilized as a ligand in metal–organic frameworks synthesis.[13d] Benzobistriazole is oxidized by potassium chromate in acidic environment to produce bistriazole-*p*-benzoquinone. Bistriazole-*p*-benzoquinone is stable up to 300 °C (Fig. S1†). It is poorly soluble in water; however, it is soluble in aqueous alkali solutions.

The room temperature solubility of H_2-btbq in a 1 M aqueous solution of LiOH, NaOH and KOH was determined by UV-Vis spectroscopy (see ESI† for details). It was found that H_2-btbq is well soluble in a 1 M LiOH solution (>100 mg mL^{-1}, *i.e.* >0.442 M), less in a 1 M KOH solution (7.94 mg mL^{-1}, *i.e.* 0.035 M) and the least in a 1 M NaOH solution (0.10 mg mL^{-1}, *i.e.* 0.4 mM). To know more about the nature of the alkali salts of H_2-btbq, attempts to obtain single crystals of the alkali salts were successfully carried out.

A suspension of H_2-btbq in water was heated and then a 2.5 M aqueous solution of the corresponding alkali hydroxide (LiOH, NaOH or KOH) was added dropwise to dissolve the linker completely. This process was accompanied by a change in colour; in all three cases, a white suspension turned into a yellow solution. Upon cooling down, in the case of the sodium and potassium salt, needle-like crystals were instantly obtained (Fig. S8†), while the lithium salt remained dissolved in the solution. The crystals of the lithium salt were obtained by a slow evaporation of the aqueous alkali solution. In all three cases, single crystals suitable for single crystal X-ray analysis were obtained, and thus the structures of the alkali salts could be elucidated.

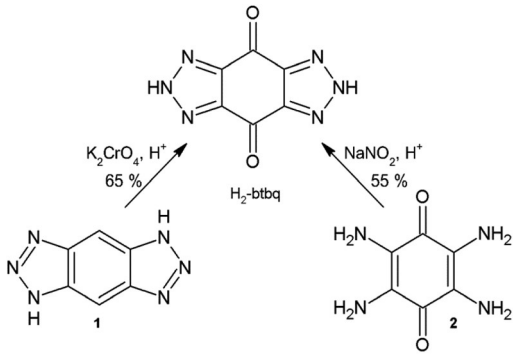

Scheme 1 Different synthesis routes to bistriazole-*p*-benzoquinone (H_2-btbq).[14,15]

Single crystal X-ray analysis

The ligand **H_2-btbq** crystallizes as a dihydrate H_2-btbq·$2H_2O$ and its crystal structure has been recently reported.[14] The crystal data and structure refinement of its alkali salts are summarized in Table 1.

Li_2-btbq·$2H_2O$ crystallizes in the monoclinic crystal system within the space group $P2_1/c$ (no. 14). The asymmetric unit consists of one lithium atom, three carbon, three nitrogen, two oxygen and two hydrogen atoms constituting half of the $btbq^{2-}$ ligand, and one water molecule. An ORTEP-style plot of the asymmetric unit of Li_2-btbq·$2H_2O$ with atom labels is shown in Fig. S10.† Li_2-btbq·$2H_2O$ features a 3-D coordination network constructed from $btbq^{2-}$ ligands, lithium cations and water molecules. The ligand molecules are stacked along the *a*-axis and create a zig-zag pattern in the *c*-direction (Fig. S11†). The lithium ions are tetrahedral coordinated by one nitrogen and one oxygen donor atoms steaming from two different ligand molecules and two oxygen atoms belonging to two water molecules (see Fig. 1). The chains of Li-tetraeders are

Table 1 Crystal data and structure refinement of alkali salts of H_2-btbq

Compound	Li_2-btbq·$2H_2O$	Na_2-btbq·$4H_2O$	K_2-btbq·$2H_2O$
Empirical formula	$C_6H_4Li_2N_6O_4$	$C_6H_8Na_2N_6O_6$	$C_6H_4K_2N_6O_4$
Formula weight	238.03	306.16	302.35
T/K	100(2)	293(2)	100(2)
λ/Å	0.71073	0.71073	0.71073
Crystal system	Monoclinic	Monoclinic	Monoclinic
Space group	$P2_1/c$ (no. 14)	$C2/c$ (no. 15)	Cc (no. 9)
a/Å	3.40910(10)	10.4329(7)	9.4207(5)
b/Å	9.2113(4)	15.5499(10)	18.4255(9)
c/Å	14.3342(7)	6.8575(4)	6.3412(3)
β/°	99.880(2)	100.221(2)	110.193(3)
Volume/Å^3	443.45(3)	1094.84(12)	1033.06(9)
Z	2	4	4
Density/mg m^{-3} (calc.)	1.783	1.857	1.944
Absorption coeff./mm^{-1}	0.146	0.226	0.937
F(000)	240	6240	608
Theta range/°	2.88 to 32.09	2.38 to 28.31	2.56 to 33.27
Measured reflections	11 739	12 452	21 639
Independent reflections/R_{int}	1543/0.0521	1367/0.0557	3751/0.0639
Data/restraints/parameters	1544/0/90	1367/2/108	3751/6/179
Goodness of fit on F^2	1.062	1.070	1.055
R_1 ($I > 2\sigma(I)$)[a]	0.0405	0.0346	0.0557
wR_2 (all data)[b]	0.0965	0.0841	0.1222
$\Delta\rho_{max,min}$/e Å^{-3}	0.497, −0.296	0.513, −0.337	0.707, −1.056

[a] $R_1 = \sum||F_o| - |F_c||/\sum|F_o|$. [b] $wR_2 = \{\sum[w(F_o^2 - F_c^2)^2]/\sum[w(F_o^2)^2]\}^{1/2}$.

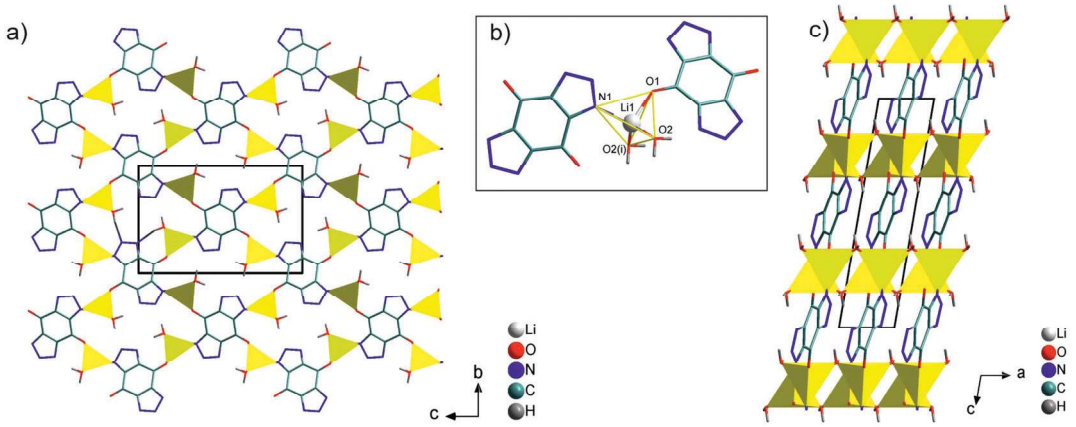

Fig. 1 Packing diagram of Li_2-btbq·$2H_2O$ with coordination polyhedra of Li-cations viewed in the *a*- (a) and *b*-direction (c), and a portion of the crystal structure of Li_2-btbq·$2H_2O$ emphasizing the coordination environment of the Li-cations (b).

expanding in the *a*-direction. The framework is further stabilized by π–π-stacking between the ligand molecules (the distance between the centroids of the benzene rings from two $btbq^{2-}$ ligands is 3.41 Å) and by hydrogen bridges formed between nitrogen atoms (acceptors) from $btbq^{2-}$ ligands and hydrogen atoms from waters molecules (donors). The atomic coordinates and isotropic thermal parameters, bond length and angles, hydrogen bonds are presented in Tables S2–5.†

Na_2-btbq·$4H_2O$ crystallizes in the monoclinic crystal system within the space group *C*2/*c* (no. 15). The asymmetric unit consists of one sodium atom, three carbon, three nitrogen, four oxygen and four hydrogen atoms constituting half of the $btbq^{2-}$ ligand, and three water molecules. An ORTEP-style plot of the asymmetric unit of Na_2-btbq·$4H_2O$ with atom labels is shown in Fig. S12.† Na_2-btbq·$4H_2O$ features a 3-D coordination network constructed from $btbq^{2-}$ ligands, sodium cations and water molecules. The sodium ions are octahedral coordinated by four oxygen atoms steaming from four different water molecules, and one oxygen and one nitrogen atoms belonging to two different ligand molecules. The compound exhibits layered structure. Between the layers created by the Na-octahedra parallel to the *ac*-plane, there are layers formed by the organic ligands. Within the Na-cation layer, the every two Na-octahedra are edge-sharing and connected with other octahedra by their corners (Fig. 2). Two water molecules ($H_2O(3)$) and ($H_2O(4)$) are located on a two-fold axis (Wyckoff notation 4*e*). The framework is further stabilized by π–π-stacking between the ligand molecules (the distance between the centroids of the benzene rings from two $btbq^{2-}$ ligands is 3.43 Å) and by hydrogen bonds. The water molecules are engaged in four different hydrogen bonds, involving one oxygen and two nitrogen donor atoms from the ligand. More precisely, the nitrogen donor atom N(2) interacts with two hydrogen atoms from two different water molecules: N(2)···H(3)–O(3): 2.43 Å and N(2)···H(4)–O(4): 2.12 Å, and the nitrogen donor atom N(1) forms a hydrogen-bonding interaction with another water molecule: N(1)···H(1)–O(2): 2.02 Å. The last hydrogen bond is formed between the oxygen donor atom (C═O) and the previous water

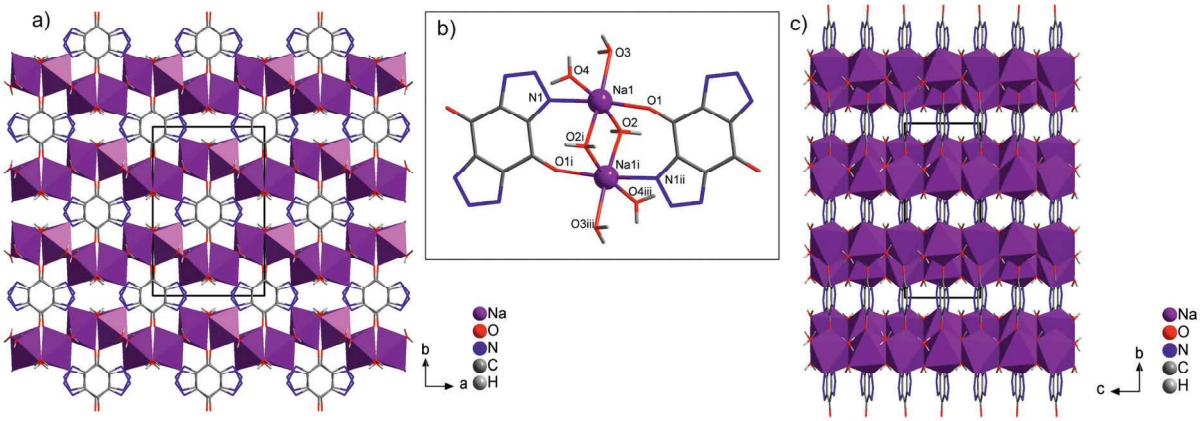

Fig. 2 Packing diagram of Na_2-btbq·$4H_2O$ with coordination polyhedra of Na-cations, view in the *c*- (a) and *a*-direction (c), and a portion of the crystal structure of Na_2-btbq·$4H_2O$ emphasizing the coordination environment of Na-cations (b). Symmetry transformations used to generate equivalent atoms: (i) (*x*, 2 – *y*, 1/2 + *z*); (ii) (1/2 + *x*, 3/2 – *y*, 1/2 + *z*); (iii) (1 – *x*, 2 – *y*, 2 – *z*).

molecule: O(1)···H(2)–O(2): 2.23 Å. The atomic coordinates and isotropic thermal parameters, bond length and angles, hydrogen bonds are presented in Tables S6–9.†

K_2-btbq·2H_2O crystallizes in the monoclinic crystal system within the space group *Cc* (no. 9). The asymmetric unit consists of two potassium atoms, six carbon, six nitrogen, four oxygen and four hydrogen atoms constituting one molecule of the $btbq^{2-}$ ligand, and two water molecules. An ORTEP-style plot of the asymmetric unit of K_2-btbq·2H_2O with atom labels is shown in Fig. S14.† The compound exhibits layered structure created by layers of potassium cations (K(2)) and water molecules, and potassium cations (K(1)) and $btbq^{2-}$ ligands. The *ac*-layers are perpendicular to the *b*-axis, whereas the organic molecules within these layers are arranged perpendicular to the *c*-axis (see Fig. 3). The two K-cations have different coordination numbers – K(1): 10 and K(2): 8 (see Fig. 3b). To the coordination sphere of K(1) belongs four oxygen atoms (two steaming from two $btbq^{2-}$ ligands and two from two water molecules) and six nitrogen atoms (belonging to three different $btbq^{2-}$ ligands). The interatomic K–O distances fall within the range of 2.757–3.338 (K(1)–O) and 2.703–2.999 (K(2)–O) Å, whereas K–N distances are in the range of 2.926–3.238 (K(1)–N) and 3.356–3.363 (K(2)–N). These distances are in good agreement with those found in the literature.[16] The framework is further stabilized by hydrogen-bond network developed through the hydrogen atoms of the water molecules and nitrogen donor atoms of the ligand, namely N(1), N(2), N(5) and N(6), and by π–π-stacking interactions between the ligand molecules. The distance between the centroids of benzene rings of the $btbq^{2-}$ ligands is equal to 3.17 Å. The atomic coordinates and isotropic thermal parameters, bond length and angles, hydrogen bonds are presented in Tables S10–13.†

Thermal stability

For practical applications, the material stability at elevated temperature is often important. Therefore, the thermal stability of the lithium, sodium and potassium salt of H_2-btbq was studied by TGA (Fig. 4) and VT-XRPD (Fig. S4†). It was shown that after removing the water molecules (the first mass loss observed by the TG analysis, Fig. 4), the compounds were stable approximately up to 400–450 °C. However, not surprisingly, in all three cases upon removing the water molecules, the crystal structure changed and the diffraction peaks moved to higher 2θ values indicating smaller unit cells (Fig. S4†).

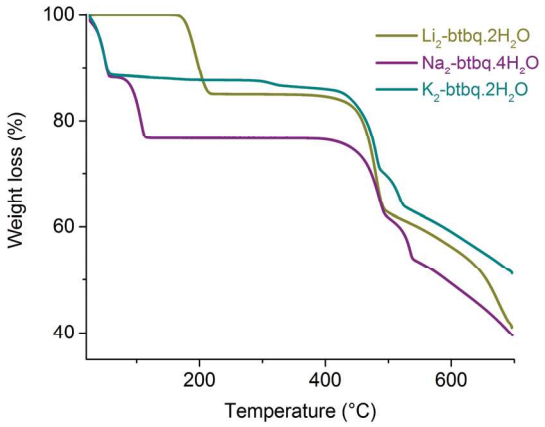

Fig. 4 Thermal stability of Li_2-btbq·2H_2O, Na_2-btbq·4H_2O and K_2-btbq·2H_2O studied by TG analysis under a nitrogen atmosphere.

The TG analysis of Li_2-btbq·2H_2O revealed two main weight loss steps. The first step at about 200 °C corresponds to the loss of the two coordinated water molecules per one Li_2-btbq molecule. The calculated mass loss is 15.12%, which matches well to the measured value of 15.05%. At about 450 °C, the compound starts to decompose. The TG curve of Na_2-btbq·4H_2O shows four weight loss steps. The two first steps can be assigned to the removal of four water molecules – two of them in each step. In the measurement 23.32% of the weight was lost, which is in good agreement with the calculated value of 23.54%. The third and fourth step is the stepwise decomposition of the ligand molecule (around 450 °C). The TG curve of K_2-btbq·2H_2O revealed three main steps. The first step corresponds to the removal of two water molecules

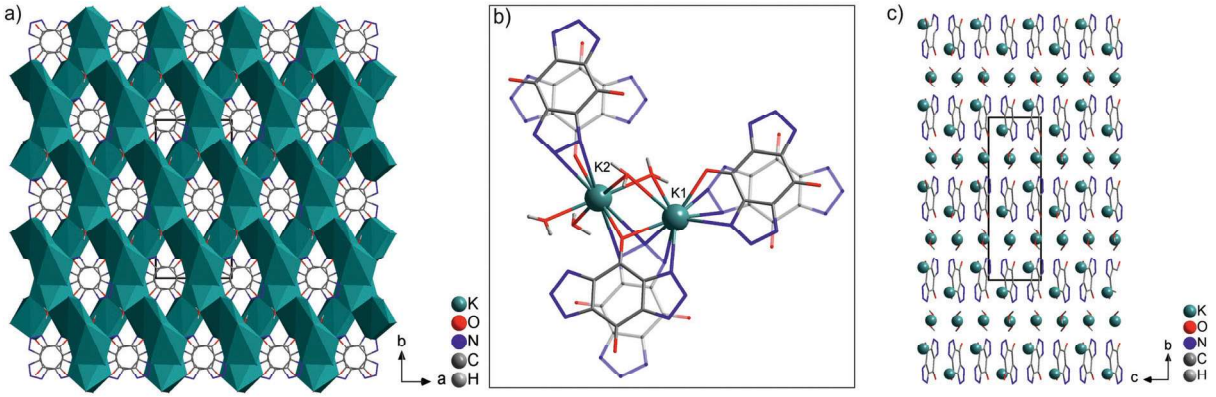

Fig. 3 Packing diagram of K_2-btbq·2H_2O with coordination polyhedra of K-cations, view in the *c*- (a) and *a*-direction (c), and a portion of the crystal structure of K_2-btbq·2H_2O emphasizing the coordination environment of K-cations (b).

per one K_2-btbq molecule (measured: 11.59%, calculated: 11.91%). The two further steps correspond to the compound decomposition around 450 °C.

Infrared spectroscopy

The presence of the *p*-quinone unit in the prepared compounds was confirmed by IR spectroscopy in which the characteristic absorption bands of carbonyl groups were detected (Fig. S3†). The IR measurements revealed the carbonyl stretching frequency in the range of 1700–1660 cm^{-1} (namely 1699 cm^{-1} for H_2-btbq·$2H_2O$, 1663 cm^{-1} for Li_2-btbq·$2H_2O$, 1673 cm^{-1} for Na_2-btbq·$4H_2O$ and 1664 cm^{-1} for K_2-btbq·$2H_2O$) which is in agreement with the previously reported IR data of substituted *p*-quinones.[17]

Electrochemical properties

The electrochemical behaviour of bistriazole-*p*-benzoquinone was investigated *via* cyclic voltammetry (CV). In aqueous alkali electrolytes (*i.e.* in 1 M LiOH, NaOH and KOH), two successive one-electron reduction waves were detected. The first electron reduction was reversible whereas the second electron reduction was quasireversible (Fig. 5 and Table 2). We suppose that the alkali cations of the supporting electrolyte form an ion pair with the semiquinone and/or quinone dianion. Additionally, the mono- and dianions can be stabilized by hydrogen bonding involving solvent water molecules. Due to the ion pair formation, reduction potentials are shifted towards positive direction in the order $Li^+ > Na^+ > K^+$ (Table 2), which is in agreement with observations reported in literature, for instance, for calix-[4]-arene diquinones after complexation with a series of metal ions.[18] As it was reported, the extent of such shift depends on the ionic potential Φ_{eff} of the cation. Φ_{eff} is defined as $z/(r + \delta)$, where z and r are the charge and Pauling's radius of cation, respectively, and δ is Latimer type correction factor.[4a] Hence, the greater charge and smaller size of a metal ion causes larger shift in the reduction potential. Therefore, the association with the di-ions decreases in the order: $Li^+ > Na^+ > K^+$. To verify the association, a CV measurement of H_2-btbq·$2H_2O$ in a 1 M aqueous solution of Bu_4NOH was carried out (Fig. 5S† and Table 2). Tetrabutylammonium is known as a non-interacting cation since it has a large effective area and therefore a smaller charge density. As expected it is then much harder to reduce the species to form the semiquinone and the di-anion compared to the measurements in alkali electrolytes (*e.g.* the anodic shifts are 86 mV and 138 mV for E_1^0 and E_2^0, respectively, in comparison to LiOH, Table S2†).

The functionalization of *p*-benzoquinone with the 1,2,3-triazolate units lowered the reduction potential (compared to non-functionalized quinones). Similar results were also observed for alkali solutions of 9,10-antraquinones functionalized with hydroxyl groups which were reported as negative electrolyte reservoirs for constructing alkaline flow batteries.[12] For that purpose, the lowering the reduction potential was a desired property because it resulted in an expansion of the battery voltage. The triazolate units are also responsible for improving the solubility. Quinones are often poorly soluble in aqueous solutions which limit their applications as battery materials. However, in our case, the triazole groups are deprotonated in the alkaline solution to provide solubility and greater electron donation capability. Especially the high solubility of bistriazole-*p*-benzoquinone in an aqueous solution of lithium hydroxide (>0.442 M) is promising regarding its potential applications as a battery material.

Results of CV measurements at different scan rates (1000, 500, 200, 100, 50, 25 and 10 mV s^{-1}) and the Randles-Sevčik plots are shown in Fig. S6 and S7,† respectively.

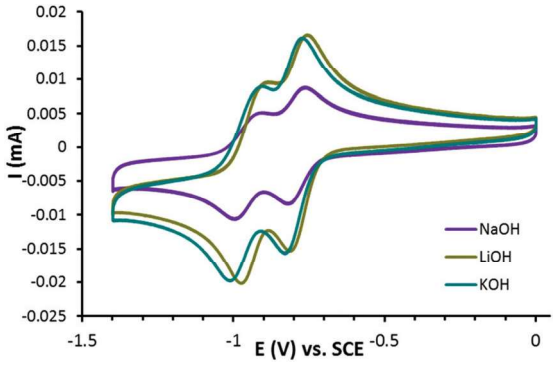

Fig. 5 Cyclic voltammograms of H_2-btbq·$2H_2O$ in a 1 M aqueous solution of LiOH, NaOH and KOH measured at room temperature at the rate of 100 mV s^{-1}.

Table 2 Redox potentials (E_1^0 and E_2^0), corresponding anodic and cathodic peak potential differences (ΔE) in different aqueous basic electrolytes

Base	E_1^0 (mV) *vs.* SCE	ΔE (mV)	E_2^0 (mV) *vs.* SCE	ΔE (mV)
LiOH	−782	57	−928	86
NaOH	−790	57	−953	88
KOH	−799	57	−958	106
Bu_4NOH	−868	58	−1066	86

Conclusions

Bistriazole-*p*-benzoquinone (H_2-btbq·$2H_2O$) was synthetized in a one-step reaction from benzobistriazole, and its electrochemical properties in alkali aqueous solutions were studied by cyclic voltammetry. It was found than the compound undergoes two successive one-electron reduction steps in the alkali solutions – the first step is reversible and the second quasireversible. This indicates that the alkali cations of the supporting electrolyte form an ion pair with the semiquinone and/or quinone dianion, and/or that the mono- and dianions are stabilized by hydrogen bonding involving solvent water molecules. Based on the nature of the alkali cation, the potential of the cathodic peak minimum and the anodic peak maximum was shifted towards positive direction as follows $Li^+ > Na^+ > K^+$ which is in agreement with the ionic potential of the cations.

To learn more about the nature of the alkali salts, H_2-btbq·$2H_2O$ was dissolved in aqueous alkali hydroxide solutions and crystallized. The structure of the corresponding alkali salts was elucidated by single crystal X-ray analysis. The lithium and potassium salts were obtained as dihydrates, Li_2-btbq·$2H_2O$ and K_2-btbq·$2H_2O$, whereas the sodium salt crystallizes as a tetrahydrate Na_2-btbq·$4H_2O$, which was confirmed not only by the single crystal X-ray analysis, but also by thermogravimetric analysis. It was shown that the compounds are thermally stable approximately up to 450 °C. However, upon removing the water molecules, their crystal structure changed as it was shown by the VT-XRPD measurements.

The benzoquinone unit was introduced to the molecular design to improve the electrochemical properties of the benzobistriazole ligand. As it was shown by the CV measurements, the prepared compound was redox-active. The functionalization of *p*-benzoquinone with the 1,2,3-triazolate units lowered the reduction potential and improved the solubility in alkali hydroxide solutions, both making the compound a promising material for constructing alkaline flow batteries. Moreover, it might be possible to use the ligand for the synthesis of coordination materials (*e.g.* MOFs) with potential redox-active properties which is in a focus of our current research.

Experimental

Materials and methods

All reagents were of analytical grade and used as received from commercial suppliers. Fourier transform infrared (FTIR) spectra were recorded in the range of 400–4000 cm^{-1} on a Bruker Equinox 55 FT-IR spectrometer equipped with an ATR unit. ^{13}C NMR spectra were recorded on a Varian 400 NMR spectrometer. Molecular masses were measured by a Q-Tof Ultima Mass spectrometer (Micromass). Thermogravimetric analysis (TGA) was performed with a TGA Q500 analyser in the temperature range of 25–700 °C under a nitrogen atmosphere at a heating rate of 5 K min^{-1}. The cyclic voltammograms were recorded on a biologic SP-300 potentiostat using a conventional three-electrode system (a glassy carbon working electrode – 3 mm in a diameter, a saturated calomel reference electrode and a platinum wire counter electrode). The experiments were carried out at room temperature at different scan rates from 1000 to 10 mV s^{-1} in a 1 M, oxygen free, aqueous solution of LiOH, NaOH, KOH and Bu_4NOH. In the case of using a solution of LiOH and KOH, 2 mg of H_2-btbq·$2H_2O$ (0.009 mmol) in 10 mL were used. In the case of using a solution of NaOH and Bu_4NOH, only 1 mg of H_2-btbq·$2H_2O$ (0.004 mmol) in 10 mL was used (higher amount was not possible to use due to the limited solubility of H_2-btbq in the solutions). X-ray powder diffraction data were collected in the 5–50° 2θ range using a Seifert XRD 3003 TT – powder diffractometer with a Meteor1D detector operating at room temperature using Cu $K_{\alpha 1}$ radiation (λ = 1.54187). VT-XRPD data were collected on a Panalytical Empyrean diffractometer in transmittance Bragg–Brentano geometry employing Cu-radiation. The patterns were recorded in a temperature range of 30 to 550 °C, in the 3–60° 2θ range with a step time of 1 s and a step width of 0.02° 2θ. Temperature program between measurements: 0.5 °C s^{-1} heating rate, followed by 10 min isothermal steps required for recording diffraction data sets. The samples were exposed to a nitrogen atmosphere during the measurements. For the single crystal X-ray analysis, the crystals of Li_2-btbq·$2H_2O$, Na_2-btbq·$4H_2O$ and K_2-btbq·$2H_2O$ were taken from mother liquor and mounted on a MiTeGen MicroMounts. The X-ray data for the single crystal structure determination were collected on a Bruker D8 Venture diffractometer. Intensity measurements were performed using monochromated (doubly curved silicon crystal) MoKα radiation (0.71073 Å) from a sealed microfocus tube. Generator settings were 50 kV, 1 mA. APEX3 software was used for preliminary determination of the unit cell.[19] Determination of integrated intensities and unit cell refinement were performed using SAINT.[20] The structure was solved and refined using the Bruker SHELXTL Software Package.[21] H-atoms of water molecules were found from the difference Fourier map. Complete crystallographic data have been deposited in the CIF format as supplementary publication no. CCDC 1561795–1561797.†

Synthesis procedures

Bistriazole-*p*-benzoquinone (H_2-btbq) and sodium bistriazole-*p*-benzoquinone (Na_2-btbq). To prepare H_2-btbq and Na_2-btbq, a procedure reported in literature was optimized.[15] Benzobistriazole (0.58 g, 3.63 mmol), prepared according to previously reported procedures,[22] was dissolved in water (10 mL) containing an aqueous solution of NaOH (2.5 M, 2 mL). The mixture was carefully acidified with sulphuric acid (66%, 10 mL) while stirred and heated up to 95 °C. Then an aqueous solution of K_2CrO_4 (3.5 g in 10 mL of water, 18.02 mmol) was added at once. Upon cooling, a precipitate formed. The beige precipitate was filtered and washed three times with 5 ml of water to yield H_2-btbq as a crude product (0.63 g). For further purification, 0.60 g of the crude product was dissolved in water (25 mL) containing an aqueous solution of NaOH (2.5 M, 3 mL). The mixture was heated to 85 °C. The resulting red solution was filtered through charcoal (a hot filtration) and the filtrate was slowly cooled to room temperature. Upon cooling, Na_2-btbq was obtained as yellow needle-like crystals. The crystals were isolated *via* filtration to give 0.62 g of Na_2-btbq·$2H_2O$ (2.03 mmol, 58.7%). IR: $\bar{\nu}$ = 3560, 3300, 3224, 1673, 1638, 1603, 1487, 1429, 1388, 1165, 1054, 1022, 979, 763, 695, 536 and 430 cm^{-1}.

To obtain H_2-btbq as a pure product, Na_2-btbq·$2H_2O$ (0.50 g, 1.63 mmol) was dissolved in water (100 mL) and the mixture was heated to 85 °C. After that, the solution was carefully acidified with HCl (32%, 2 mL). The color of the solution turned from yellow to colorless. Upon cooling, a white precipitated formed. The precipitate was isolated *via* filtration and washed well with water to yield H_2-btbq·$2H_2O$ (0.34 g, 92.1%) as a white solid. ^{13}C NMR (125.7 MHz, C_2D_6OS, 20 °C): δ = 176.00 (aromatic, ketone), 147.40 (aromatic); IR: $\bar{\nu}$ = 3513,

3457, 1699, 1612, 1510, 1482, 1396, 1374, 1349, 1182, 1130, 1052, 1022, 978, 925, 754, 716, 694, 672 and 447 cm^{-1}; MS (ESI^-): *m*/*z* (%): 211.01 (100) $[M - Na]^-$; MS (HR-ESI): *m*/*z* 211.0003, $[C_6N_6O_2Na_2]$ requires 210.9986.

Lithium bistriazole-*p*-benzoquinone (Li_2-btbq). H_2-btbq·$2H_2O$ (0.34 g, 1.50 mmol) and LiOH (0.07 g, 2.92 mmol) were mixed in water (5 mL). The resulting mixture was heated to 80 °C, so that both compounds dissolved to form a yellow transparent solution. Then the stirring of the solution was stopped, and the solvent was slowly evaporated to give Li_2-btbq·$2H_2O$ (0.30 g, 1.26 mmol, 83.8%). IR: $\bar{\nu}$ = 3432, 3105, 1663, 1584, 1552, 1496, 1433, 1397, 1197, 1172, 1088, 1040, 997, 806, 760, 707, 691, 572 and 440 cm^{-1}.

Potassium bistriazole-*p*-benzoquinone (K_2-btbq). K_2-btbq was synthesized in the same way as Na_2-btbq, except that KOH was used instead of NaOH. Upon cooling, K_2-btbq·$2H_2O$ (0.16 g, 0.53 mmol, 15.3%) was obtained as yellow needle-like crystals. The reaction yield of K_2-btbq was lower compared to the Na_2-btbq (58.7%) due to the higher solubility of K_2-btbq in water. IR: $\bar{\nu}$ = 3320, 3172, 1664, 1534, 1486, 1422, 1412, 1385, 1165, 1053, 1018, 973, 760, 699, 599 and 449 cm^{-1}.

Conflicts of interest

The authors declare no conflicts of interest.

Acknowledgements

HB is grateful to the program “Chancengleichheit für Frauen in Forschung und Lehre” from the University of Augsburg for financial support *via* a fellowship.

References

1 (*a*) R. A. C. Tomé, in *Science of Synthesis Category 2, Hetarenes and Related Ring Systems*, ed. R. C. Storr and T. L. Gilchrist, Georg Thieme Verlag KG, Stuttgart, Germany, 2003, vol. 13, p. 415; (*b*) E. A. Shafran, V. A. Bakulev, Y. A. Rozin and Y. M. Shafran, *Chem. Heterocycl. Compd.*, 2008, **44**, 1040; (*c*) S. Haider, M. S. Alam and H. Hamid, *Inflammation Cell Signaling*, 2014, e95.

2 A. R. Katritzky and B. V. Rogovoy, *Chem. – Eur. J.*, 2003, **9**, 4586.

3 (*a*) Y. Bourne, H. C. Kolb, Z. Radic, K. B. Sharpless, P. Taylor and P. Marchot, *Proc. Natl. Acad. Sci. U. S. A.*, 2004, **101**, 1449; (*b*) A. R. Katritzky, X. Lan, J. Z. Yang and O. L. Denisko, *Chem. Rev.*, 1998, **98**, 409.

4 (*a*) P. S. Guin, S. Das and P. C. Mandal, *Int. J. Electrochem.*, 2011, 816202; (*b*) J. Q. Chambers, in *The Quinonoid Compounds*, ed. S. Patai and Z. Rappoport, John Wiley & Sons, Inc., Chichester, UK, 1988, vol. 12, p. 719.

5 W. A. Cramer, in *Energy Transduction in Biological Membranes*, ed. C. R. Cantor, Springer-Verlag, New York, USA, 1990, vol. 5, p. 193.

6 I. Abraham, R. Joshi, P. Pardasani and R. T. Pardasani, *J. Braz. Chem. Soc.*, 2011, **22**, 385.

7 J. Madeo, A. Zubair and F. Marianne, *SpringerPlus*, 2013, **2**, 139.

8 P. S. Guin, S. Das and P. C. Mandal, *Int. J. Electrochem. Sci.*, 2008, **3**, 1016.

9 M. Quan, D. Sanchez, M. F. Wasylkiw and D. K. Smith, *J. Am. Chem. Soc.*, 2007, **129**, 12847.

10 (*a*) E. J. Son, J. H. Kim, K. Kim and C. B. Park, *J. Mater. Chem. A*, 2016, **4**, 11179; (*b*) M. Miroshnikov, K. P. Divya, G. Babu, A. Meiyazhagan, L. M. R. Arava, P. M. Ajayan and G. John, *J. Mater. Chem. A*, 2016, **4**, 12370; (*c*) T. B. Schon, B. T. McAllister, P.-F. Li and D. S. Seferos, *Chem. Soc. Rev.*, 2016, **45**, 6345; (*d*) W. Xu, A. Read, P. K. Koech, D. Hu, C. Wang, J. Xiao, A. B. Padmaperuma, G. L. Graff, J. Liu and J.-G. Zhang, *J. Mater. Chem.*, 2012, **22**, 4032; (*e*) A.-L. Barres, J. Geng, G. Bonnard, S. Renault, S. Gottis, O. Mentre, C. Frayret, F. Dolhem and P. Poizot, *Chem. – Eur. J.*, 2012, **18**, 8800.

11 B. Huskinson, M. P. Marshak, C. Suh, S. Er, M. R. Gerhardt, C. J. Galvin, X. Chen, A. Aspuru-Guzik, R. G. Gordon and M. J. Aziz, *Nature*, 2014, **505**, 195.

12 K. Lin, Q. Chen, M. R. Gerhardt, L. Tong, S. B. Kim, L. Eisenach, A. W. Valle, D. Hardee, R. G. Gordon, M. J. Aziz and M. P. Marshak, *Science*, 2015, **349**, 1529.

13 (*a*) P. Schmieder, M. Grzywa, D. Denysenko, M. Hambach and D. Volkmer, *Dalton Trans.*, 2015, **44**, 13060; (*b*) P. Schmieder, D. Denysenko, M. Grzywa, B. Baumgärtner, I. Senkovska, S. Kaskel, G. Sastre, L. van Wüllen and D. Volkmer, *Dalton Trans.*, 2013, **42**, 10786; (*c*) D. Denysenko, M. Grzywa, M. Tonigold, B. Streppel, I. Krkljus, M. Hirscher, E. Mugnaioli, U. Kolb, J. Hanss and D. Volkmer, *Chem. – Eur. J.*, 2011, **17**, 1837; (*d*) S. Biswas, M. Grzywa, H. P. Nayek, S. Dehnen, I. Senkovska, S. Kaskel and D. Volkmer, *Dalton Trans.*, 2009, 6487.

14 M. Sato, T. Takeda, N. Hoshino and T. Akutagawa, *CrystEngComm*, 2017, **19**, 910.

15 F. Muzik and Z. J. Allan, *Collect. Czech. Chem. Commun.*, 1957, 474.

16 R. Podgajny, D. Pinkowicz, B. Czarnecki, M. Kozieł, S. Chorąży, M. Wis, W. Nitek, M. Rams and B. Sieklucka, *Cryst. Growth Des.*, 2014, **14**, 4030.

17 M.-L. Josien, N. Fuson, J.-M. Lebas and T. M. Gregory, *J. Chem. Phys.*, 1953, **21**, 331.

18 H. Kim, D. Choi, T. D. Chung, S. K. Kang, S. K. Lee, T. Kim and S.-K. Chang, *J. Electroanal. Chem.*, 1995, **387**, 133.

19 *APEX3 Version 2016.9*, Bruker AXS Inc., 2016.

20 *SAINT Version 8.37A*, Bruker AXS Inc., 2015.

21 G. M. Sheldrick, *Acta Crystallogr., Sect. C: Cryst. Struct. Commun.*, 2015, **71**, 3.

22 H. Hart and D. Ok, *J. Org. Chem.*, 1986, **51**, 979.